

Article

Quantitative Risk Assessment of Hydrogen Refueling Station in Cheonan City of South Korea

Bo-il Jeon ^{1,†}, Shinji Kim ^{1,†}, Yeo Song Yoon ^{2,*} and Seungho Jung ^{1,*} ¹ Department of Environmental and Safety Engineering, Ajou University, Suwon 16499, Republic of Korea² Department of Safety & Environmental Engineering of Graduate School, Korea University of Technology & Education, Cheonan 31253, Republic of Korea

* Correspondence: ysyoon@koreatech.ac.kr (Y.S.Y.); processsafety@ajou.ac.kr (S.J.)

† These authors contributed equally to this work.

Abstract: The average temperature of the Earth has risen due to the accumulation of greenhouse gases emitted from the usage of fossil fuels. The consequential climate changes have caused various problems, fueling the growing demand for environmentally friendly energy sources that can replace fossil fuels. Batteries and hydrogen have thus been utilized as substitute energy sources for automobiles to reduce fossil fuel consumption. Consequently, the number of hydrogen refueling stations is increasing due to an increase in the number of hydrogen-powered vehicles. However, several incidents have been reported in the United States of America and Japan where hydrogen refueling stations have been operating for a long time. A risk assessment of hydrogen refueling stations operating in urban areas was performed in this study by calculating the risk effect range using a process hazard analysis tool (PHA_{ST}) v8.7 from DNV-GL and a hydrogen risk assessment model (HyRAM) from Sandia National Laboratories (SNL). The societal risk was assessed through a probit model based on the calculation results. The assessment results showed that the risk caused by jet fire and overpressure in an incident is lower than the ‘as low as reasonably practicable’ (ALARP) level.

Keywords: hydrogen refueling station; HyRAM; PHAST; quantitative risk assessment; probit model



Citation: Jeon, B.-i.; Kim, S.; Yoon, Y.S.; Jung, S. Quantitative Risk Assessment of Hydrogen Refueling Station in Cheonan City of South Korea. *Energies* **2023**, *16*, 7138. <https://doi.org/10.3390/en16207138>

Academic Editor: Pål Østebø Andersen

Received: 16 September 2023

Revised: 8 October 2023

Accepted: 12 October 2023

Published: 18 October 2023



Copyright: © 2023 by the authors. Licensee MDPI, Basel, Switzerland. This article is an open access article distributed under the terms and conditions of the Creative Commons Attribution (CC BY) license (<https://creativecommons.org/licenses/by/4.0/>).

1. Introduction

The consumption of fossil fuel has increased drastically since its recognition as one of the main sources of energy for humankind. The emission of greenhouse gases has concomitantly increased, leading to an increase in the average temperature of the Earth. Climate changes due to the rise in the Earth’s average temperature have resulted in a variety of issues, thus highlighting the importance of reducing the use of fossil fuels and increasing the utilization of environmentally friendly energy sources. One well-known way of reducing the usage of fossil fuels is by changing the type of fuels used for automobiles. The European Union (EU) announced the decision to limit the operation of automobiles powered by fossil fuels. Batteries and hydrogen are widely used as substitute power sources for automobiles in place of fossil fuels [1]. Thus, the number of hydrogen-powered automobiles is constantly increasing. According to statistical data from the Ministry of Land, Infrastructure, and Transport, the number of hydrogen-powered vehicles registered in Korea increased by nearly three-fold, from 11,046 in January 2021 to 32,484 in June 2023 [2]. The number of hydrogen refueling stations (HRSs) is increasing due to an increase in the number of hydrogen-powered vehicles. Hydrogen refueling stations are operated mainly in Asian countries such as South Korea, Japan, and China. In European countries, HRSs are operated in Germany, France, the United Kingdom, the Netherlands, and Switzerland. Globally, more than 1070 HRSs have been built as of 2023, of which, 210 HRSs are located in South Korea [3].

Hydrogen refueling stations for HFCVs (Hydrogen Fuel Cell Vehicles) have the advantage of faster charging than electric vehicle charging stations for electric vehicles. Hydrogen

vehicles do not generate greenhouse gases in the process of generating power. In addition, hydrogen has the advantage of having a higher calorific value per unit mass than fossil fuels. On the contrary, hydrogen has a very low ignition energy of 0.018 mJ and a wide combustion range of 4–75% in the air. Because hydrogen has a low energy per unit volume, it is stored at high pressure to increase its energy density [4]. When hydrogen is leaked from a high-pressure storage facility through a leak hole, a shock wave compresses the air and the temperature of the hydrogen–air mixture rises. Then, self-ignition may occur [5,6]. This phenomenon increases the risk associated with storage tanks and tube trailers used at HRSs.

No accidents involving HRSs have occurred in South Korea thus far, but several cases have been reported in the U.S. and Japan where HRSs have been operating for years. In the U.S., 22 incidents occurred from 2004 to 2012, whereas in Japan, 21 incidents occurred from 2005 to 2014 [7]. Since there is a risk of high-pressure hydrogen and an accident risk of HRSs, it is necessary to evaluate the risk of high-pressure hydrogen facilities in HRSs. Accordingly, several prior studies have focused on the quantitative risk assessment (QRA) of high-pressure facilities in HRSs [8–10]. However, most of these studies assessed individual risks of HRSs. This study thus aims to evaluate the risk of an HRS that is currently operational and to lower the societal risk of it.

2. Materials and Methods

This study assessed the safety of hydrogen refueling stations installed in urban regions of Korea. A consequence analysis (CA) and a QRA were performed based on the information from the HRS analyzed in this study.

2.1. Scenario

2.1.1. HRS Specifications

The analyzed HRS was selected because it has a high individual risk as it handles a large amount of hydrogen and there is a high population density in the installation area and a high societal risk in the nearby residential areas in the case of hydrogen leakage. The HRS analyzed in this study is in Cheonan City in South Korea. Residential and commercial regions are located 100 m to the west from the HRS. Table 1 presents the specifications for a tube trailer and a storage tank used at the analyzed HRS, while Figure 1 illustrates the process flow diagram (PFD) of the HRS. The analyzed HRS uses a tube trailer pressurized to 350 bar and a storage tank pressurized to 850 bar and refuels hydrogen automobiles at a pressure of 700 bar through a dispenser.

Table 1. HRS specifications.

Components	Tube Trailer	Storage Tank
Pressure (bar)	350	850
Operating Temperature (°C)	20	20
Hydrogen Mass (kg)	234	750

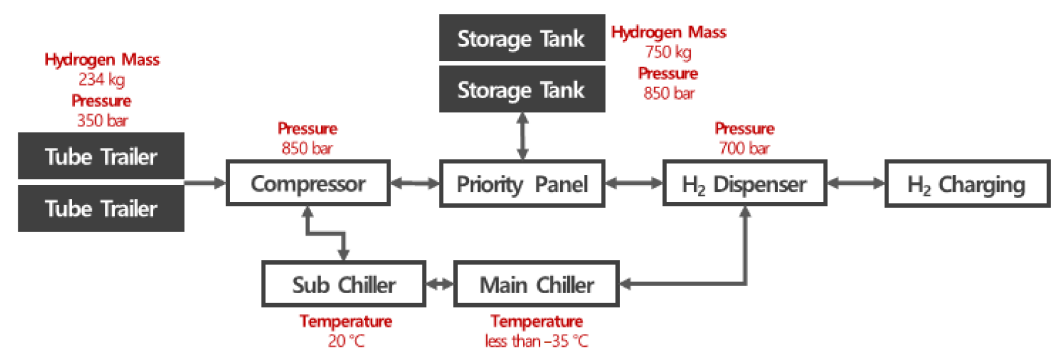


Figure 1. Process flow diagram (PFD) of HRS.

Figure 2 shows the location of the HRS and a description of the surrounding region. A wide road is located to the west of the HRS, followed by residential areas. Commercial facilities are located between the two residential areas. A parking facility is located to the north and the east of the HRS, and a park is situated to the south of the HRS.



Figure 2. Location and regional status of the HRS.

2.1.2. Accident Scenario

The factors (leak size and leak frequency) required to devise an accident scenario for the HRS were referenced from the “Analyses to Support Development of Risk-Informed Separation Distances for Hydrogen Codes and Standards” of Sandia National Laboratories (SNL) [11]. Table 2 presents three types of leak sizes and leakage frequencies proposed in the SNL standard, appropriate for the design pressure of the analyzed HRS.

Table 2. Accident scenario data for HRS.

Components		Tube Trailer	Storage Tank
Leak size (mm)	Small	1.27	0.72
	Medium	4.02	2.26
	Large	12.7	7.16
Leakage frequency (/year)	Small	4.14×10^{-4}	1.23×10^{-3}
	Medium	3.21×10^{-4}	2.09×10^{-4}
	Large	1.80×10^{-4}	1.02×10^{-4}

2.1.3. Weather Conditions

The atmospheric and weather conditions of the worst-case scenario were selected based on the “Technical Guideline for the Selection of Worst and Alternative Accident Scenarios” of the Korea Occupational Safety & Health Agency. Table 3 presents the wind speed, atmospheric temperature, atmospheric stability, and humidity in the worst-case weather conditions.

Table 3. Weather conditions [12].

	Wind Speed	Atmospheric Temperature	Atmospheric Stability	Humidity
Condition	1.5 m/s	40 °C	F	50%

2.2. Hydrogen Risk Analysis

The ‘risk effects’ from accidents at an HRS include thermal radiation from a jet fire and overpressure from explosions. The HyRAM 5.0 program was used to select the effect

range of a jet fire. HyRAM software was developed specifically for the modeling and QRA of hydrogen, methane, and propane systems. Certain studies have been conducted on gas leakage and jet fire modeling in hydrogen storage facilities using HyRAM [13,14]. The effect of overpressure was assessed using the process hazard analysis tool (PHASt) v8.7 of DNV-GL. PHAST is capable of modeling the leakage and dispersion of various chemical substances, as well as fire and explosion, and has been used in numerous studies for analyzing the effect of the blast overpressure of chemical substances [15].

2.2.1. Jet Fire

Jet fire can be caused by the combustion of a leaked gas stored under high pressure [16]. HyRAM provides five types of notional nozzle models [17–21]. Specifically, this study used the model proposed by Yüceil and Ötügen [17]. The conservation of mass for the notional nozzle models is represented by Equation (1).

$$\rho_{\text{eff}} v_{\text{eff}} A_{\text{eff}} = \rho_{\text{throat}} v_{\text{throat}} A_{\text{throat}} C_D \quad (1)$$

Here, ρ is the density, v is the velocity, A is the cross-sectional area, and C_D is the discharge coefficient. In the model proposed by Yüceil and Ötügen, momentum and energy are conserved as shown in Equation (2).

$$\rho_{\text{eff}} v_{\text{eff}}^2 A_{\text{eff}} = \rho_{\text{throat}} v_{\text{throat}}^2 A_{\text{throat}} C_D + A_{\text{throat}} (P_{\text{throat}} - P_{\text{throat}}) \quad (2)$$

Here, P represents the pressure. Based on Equations (1) and (2), v_{eff} can be expressed as Equation (3).

$$v_{\text{eff}} = v_{\text{throat}} C_D + \frac{P_{\text{throat}} - P_{\text{ambient}}}{\rho_{\text{throat}} v_{\text{throat}} C_D} \quad (3)$$

A_{eff} can be expressed as Equation (4).

$$A_{\text{eff}} = \frac{\rho_{\text{throat}} v_{\text{throat}}^2 A_{\text{throat}} C_D^2}{\rho_{\text{eff}} (P_{\text{throat}} - P_{\text{throat}} + \rho_{\text{throat}} v_{\text{throat}}^2 C_D^2)} \quad (4)$$

For computing the effective density to select the area in Equation (4), the density can be calculated through the conservation of energy using Equation (5) based on the assumption of isentropic expansion.

$$\frac{v_{\text{eff}}}{2} + h(\rho_{\text{eff}}, P_{\text{ambient}}) = \frac{v_{\text{throat}}^2}{2} + h_{\text{throat}} \quad (5)$$

The ‘effect range’ for humans exposed to a jet fire was determined based on three levels of thermal radiation caused by the jet fire: 4, 12.5, and 37.5 kW/m². Table 4 presents the effects of each thermal radiation range on humans.

Table 4. Effects of thermal radiation on humans [22,23].

Thermal Radiation (kW/m ²)	Effects on Humans
4	Causes pain if the duration is longer than 20 s
12.5	Fatalities within minutes
37.5	Instantaneous death

2.2.2. Overpressure

An explosion can be triggered by combustion when a leak hole is generated in a hydrogen storage tank. In this study, the risk was assessed based on the assumption that overpressure is caused by an explosion when a flash fire is generated due to ignition delay after a leak hole is created. PHAST v8.7 was used to assess the effect range of an explosion based on the TNO multi-energy (TNO ME) model [24]. The TNO ME model

is a practical model that adequately represents the mechanics of vapor cloud explosion (VCE) [25]. Figure 3 shows the basic form of the TNO ME model.

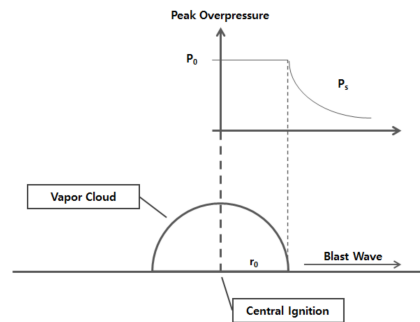


Figure 3. Basic form of vapor cloud expansion as basis of multi-energy model.

Here, P_0 is the peak overpressure and r_0 is the initial radius. The overpressure and distance can be expressed in terms of dimensionless parameters, as shown in Equations (6)–(8).

$$P'_s = \frac{\Delta P_s}{P_a} t \quad (6)$$

$$P'_{\text{dyn}} = \frac{P_{\text{dyn}}}{P_a} \quad (7)$$

$$r' = \frac{r}{\left(\frac{E}{P_a}\right)^{1/3}} \quad (8)$$

Here, P_s is the maximum blast overpressure, P_a is atmospheric pressure, r is the explosion radius, and E is the emission energy of the explosion. The scaled overpressure can be calculated by quantifying E and applying it to the overpressure curvature shown in Figure 4 according to the scaled distance (r').

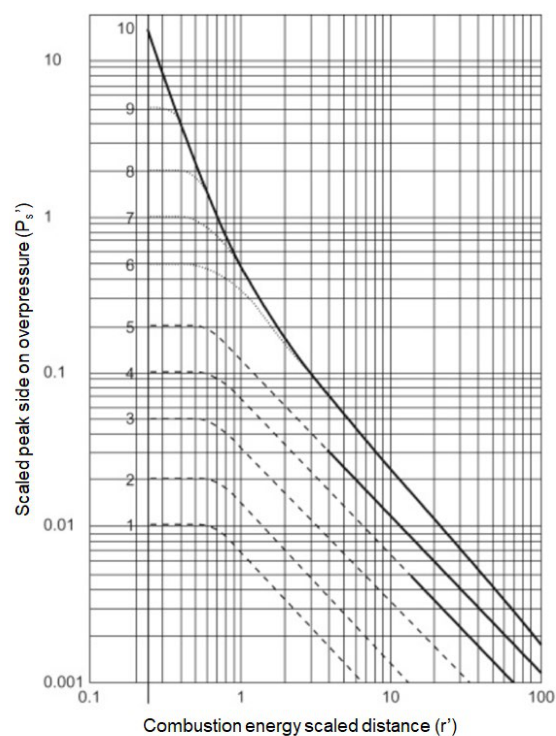


Figure 4. Peak dynamic overpressure for combustion energy scaled distance.

The contour level of the overpressure was set to 1, 3, and 5 psi according to the effects on humans. Table 5 presents the effects of different levels of overpressure on humans.

Table 5. Effects of overpressure on humans [26].

Overpressure (psi)	Effects on Humans
1	Light injuries from fragments
3	Serious injuries are common; fatalities may occur
5	Injuries are universal; fatalities are widespread

2.3. Societal Risk Analysis Method

2.3.1. Event Tree Analysis (ETA)

The physical consequences of the continuous leakage of combustible fuels such as hydrogen include gas release, jet fire, flash fire, and explosion [27,28]. Figure 5 illustrates the event sequence diagram (ESD) for each physical consequence.

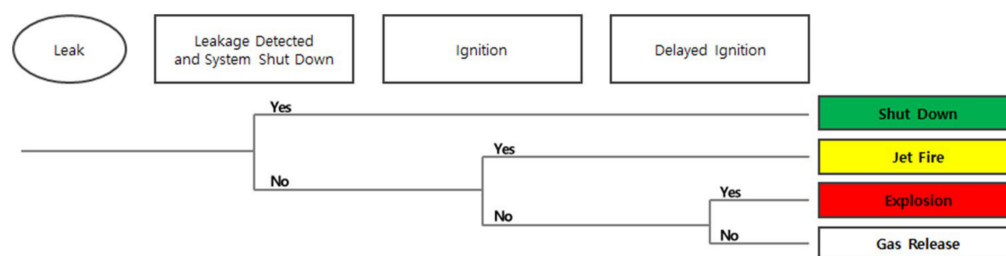


Figure 5. Event sequence diagram (ESD) [29].

The annual frequency of release is calculated for each physical consequence based on the ESD. The probability of failed leakage detection was set to 0.01 based on the probability of failure based on the demand of the system from the RVIM Guideline for Quantitative Risk Assessment, also known as the “Purple Book” [30]. The probability of hydrogen ignition according to the release rate provided by the SNL was used as the basic ignition probability, as presented in Table 6.

Table 6. Ignition probabilities for hydrogen [31].

Release Rate (kg/s)	Ignition Probability	
	Immediate	Delayed
<0.125	0.008	0.004
0.125–6.25	0.053	0.027
>6.25	0.230	0.120

2.3.2. Probit Model

A probit model is used to calculate the fatality rate of the exposed population with respect to the degree of exposure. The probit function for the acute toxicity of chemicals based on the probit model is widely utilized in the Netherlands’ external safety policy [32]. In addition, there are probit functions for thermal harm, overpressure harm, and the effects of fragments. The basic form of the probit function is shown in Equation (9).

$$Pr = k_1 + k_2 \times \ln(V) \tag{9}$$

Here, k_1 and k_2 are constants; V represents the degree and time of exposure.

For the fatality rate of heat flux, the probit function of lethality shown in Equation (10) was used in the statistical model of TNO to estimate injury due to heat radiation [24].

$$Pr_{Heat} = -36.38 + 2.56 \times \ln(t \times Q^{4/3}) \quad (10)$$

The probit function of the lung hemorrhage model due to overpressure shown in Equation (11) was used to calculate the fatality rate due to overpressure [33].

$$Pr_{Overpressure} = 1.47 + 1.37 \times \ln(P_s) \quad (11)$$

The effect range was calculated by simulating jet fire and explosion overpressure in an accident scenario. The number of fatalities for each accident scenario was calculated by applying the fatality rate derived from the probit function to the floating population of the relevant region. The F-N curve was constructed by applying the accident frequency for each scenario, calculated through ETA, to the estimated number of fatalities for assessing the societal risk.

3. Results

3.1. Results in the Case of a Jet Fire

The effect range of a jet fire was modeled using HyRAM. The heat flux at a height of 1 m and at the center of the jet fire was calculated at twenty different points from 0.01 m to 40 m (Tables 7 and 8). Referring to Table 4, the range of heat flux for 4, 12.5, and 37.5 kW/m², which is the effect on humans, was confirmed.

Table 7. Heat flux of jet fire for tube trailer.

Distance (m)	Heat Flux (kW/m ²)		
	Small Leak	Medium Leak	Large Leak
0.01	3.23	11.06	27.99
0.5	4.83	15.24	36.01
1	6.66	20.53	45.99
3	5.22	46.28	93.85
5	0.99	76.87	147.68
8	0.25	98.42	244.22
10	0.14	19.79	334.53
12	0.09	5.56	481.13
14	0.06	2.76	785.32
16	0.05	1.66	2046.52
17	0.04	1.35	2789.11
18	0.03	1.22	8114.40
19	0.03	0.94	1599.15
20	0.03	0.80	967.44
22	0.02	0.60	469.06
25	0.02	0.42	172.58
27	0.01	0.34	89.95
30	0.01	0.26	36.90
35	0.01	0.17	12.75
40	0.01	0.12	6.44

For a tube trailer, it was discovered that the heat flux exceeded 4 kW/m² for up to 3 m in the event of a small-sized leak and would thus affect humans. The heat flux exceeded 12 kW/m² for up to 10 m and exceeded 4 kW/m² for up to 12 m in the event of a medium-sized leak. For a large-sized leak, the heat flux exceeded 37.5 kW/m² for up to 27 m and exceeded 4 kW/m² at 40 m, thus affecting humans at all twenty points.

Table 8. Heat flux of jet fire in storage tank.

Distance (m)	Heat Flux (kW/m ²)		
	Small Leak	Medium Leak	Large Leak
0.01	2.59	9.63	25.35
0.5	3.88	13.48	32.91
1	5.20	18.34	42.34
3	2.32	41.57	87.56
5	0.51	64.84	138.65
8	0.14	19.22	232.94
10	0.08	4.74	327.19
12	0.05	2.18	493.88
14	0.04	1.26	916.83
16	0.03	0.82	4934.36
17	0.02	0.69	7296.73
18	0.02	0.58	1702.80
19	0.02	0.50	807.08
20	0.02	0.43	437.55
22	0.01	0.33	150.71
25	0.01	0.24	36.85
27	0.01	0.19	19.07
30	0.01	0.15	9.78
35	0.00	0.10	4.68
40	0.00	0.07	2.77

For a storage tank, it was discovered that when a small-sized leak occurred, the heat flux was 4 kW/m² or below at a distance of 3 m, thus having a low impact on humans. In the case of a medium-sized leak, the heat flux exceeded 4 kW/m² at a distance of up to 10 m, thus having an effect on humans. For a large-sized leak, the heat flux exceeded 37.5 kW/m² at distances up to 22 m and exceeded 36.85 kW/m² at 25 m, thus having a fatal impact on humans at a distance of up to 25 m.

The impact range of the heat flux was greater in a tube trailer than in a storage tank with hydrogen under very high pressure. This difference is attributable to the fact that the leak hole size of a tube trailer is set to be larger than that of a storage tank. For both the tube trailer and the storage tank, people within 3 m were exposed to the heat flux caused by a jet fire and were slightly affected when a small-sized leak occurred, but no serious injury or fatal effect was found. When a medium-sized leak occurred, however, people within 10 m of a tube trailer and 8 m of a storage tank could be killed within a few minutes. When a large-sized leak occurred, the heat flux (exceeding 37.5 kW/m²) caused by a jet fire had a fatal impact for up to 27 m for a tube trailer and up to 22 m for a storage tank.

3.2. Results in the Case of Overpressure

Table 9 presents the overpressure determined through simulation using PHAST. The simulation data from PHAST did not take the geographical features and firewalls of the HRS into account. No explosion occurred in the event of a small-sized leak, whereas overpressure of 1 psi or above occurred in the case of medium- and large-sized leaks.

For a tube trailer, the range for an overpressure of 3 psi, which can cause serious injury to people, was 8.29 m for a medium-sized leak and 30.49 m for a large-sized leak. The range for an overpressure of 5 psi, which can cause fatalities, was 6.01 m for a medium-sized leak and 22.12 m for a large-sized leak. For a storage tank, the range for an overpressure of 3 psi was 6.45 m for a medium-sized leak and 24.73 m for a large-sized leak, while the range for an overpressure of 5 psi was 4.68 for a medium-sized leak and 17.94 m for a large-sized leak. The risk range was greater in a tube trailer where the leak size was set to be larger than that in a storage tank having higher storage pressure, which is similar to the results of the jet fire simulation.

Table 9. Overpressure data.

Equipment	Leak Size	Overpressure	
		Level (psi)	Diameter (m)
Tube trailer	Medium	1	19.34
		3	8.29
		5	6.01
	Large	1	71.14
		3	30.49
		5	22.12
Storage tank	Medium	1	15.05
		3	6.45
		5	4.68
	Large	1	57.69
		3	24.73
		5	17.94

3.3. Evaluation of Fatality through Probit Model

The percentage of fatalities was calculated according to distance in each scenario using the probit function (Figures 6–9).

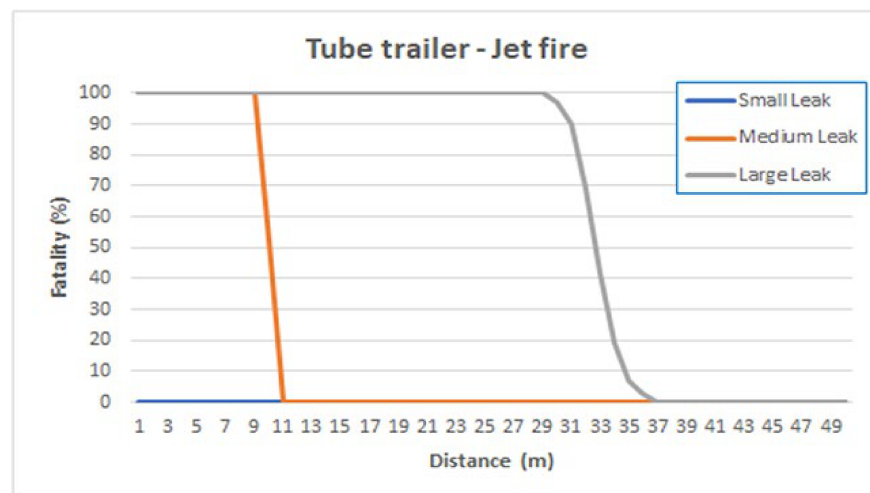


Figure 6. Fatality due to thermal radiation from jet fire at tube trailer.

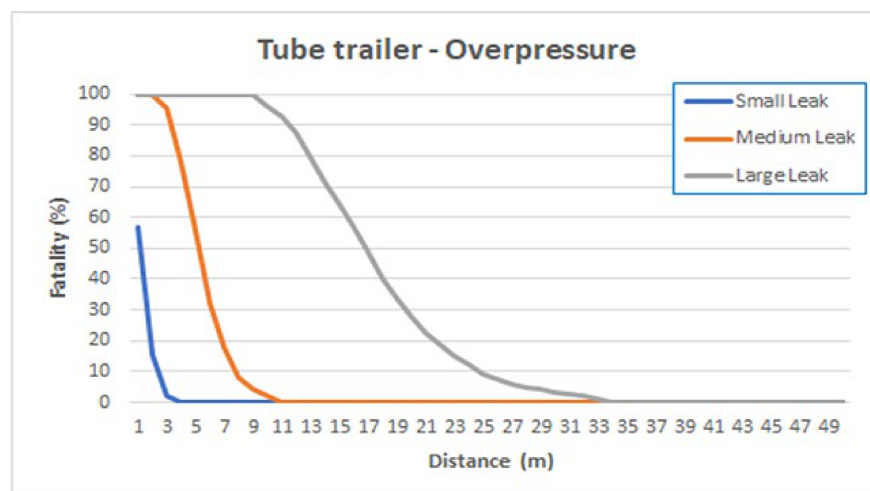


Figure 7. Fatality due to thermal radiation from overpressure at tube trailer.

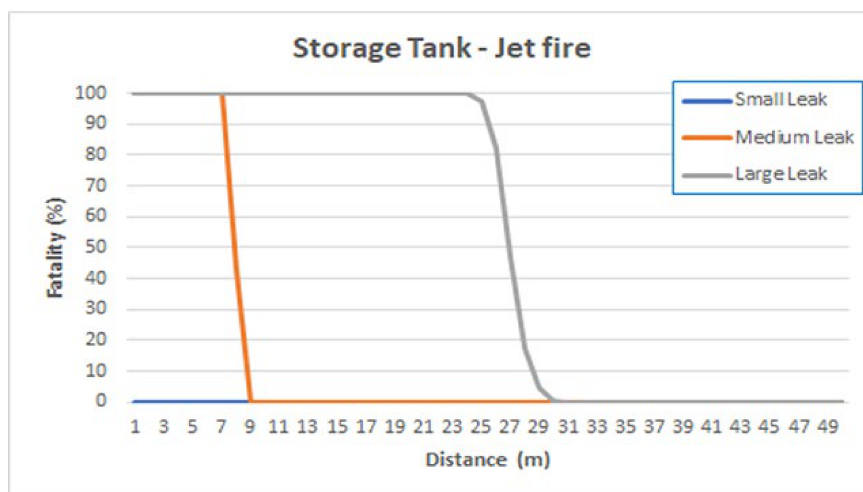


Figure 8. Fatality due to thermal radiation from jet fire at storage tank.

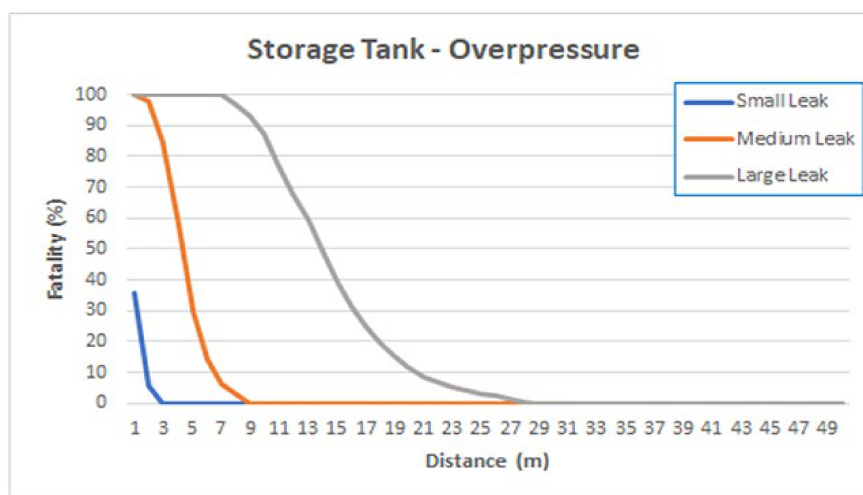


Figure 9. Fatality due to thermal radiation from overpressure at storage tank.

In accidents involving a tube trailer, the maximum distance at which fatalities may have occurred was 36 m for a jet fire and 33 m for overpressure. The maximum distance at which fatalities may have occurred in accidents involving a storage tank was 29 m for a jet fire and 27 m for overpressure.

3.4. Societal Risk

Table 10 presents the calculated frequency of jet fires and flash fires with respect to the leak size in a tube trailer and a storage tank.

Table 10. Frequency of fire in each scenario.

Equipment	Leak Size	Frequency (/Year)	
		Jet Fire	Flash Fire
Tube trailer	Small	3.33×10^{-8}	1.64×10^{-8}
	Medium	1.70×10^{-7}	8.21×10^{-8}
	Large	9.54×10^{-8}	4.60×10^{-8}
Storage tank	Small	9.84×10^{-8}	4.88×10^{-8}
	Medium	1.11×10^{-7}	5.34×10^{-8}
	Large	5.41×10^{-8}	2.61×10^{-8}

The floating population near the HRS evaluated herein was analyzed using the commercial area analysis system provided by the Ministry of SMEs and Startups [34]. The floating population was estimated by this particular system in increments of 50 m² based on the call volumes of mobile phones. Table 11 shows the floating population within 300 m of the analyzed HRS by time period as of April 2023.

Table 11. Floating population around the HRS.

Time Period	0–6	06–11	11–14	14–17	17–21	21–24	Total
Population	467	1832	1516	1649	2254	746	8464
Ratio (%)	5.5	21.6	17.9	19.5	26.6	8.8	100

The societal risk assessment was performed with the assumption that the risk is highest between 17:00 and 21:00 when the floating population is the highest; Figure 10 shows the resulting F-N curve.

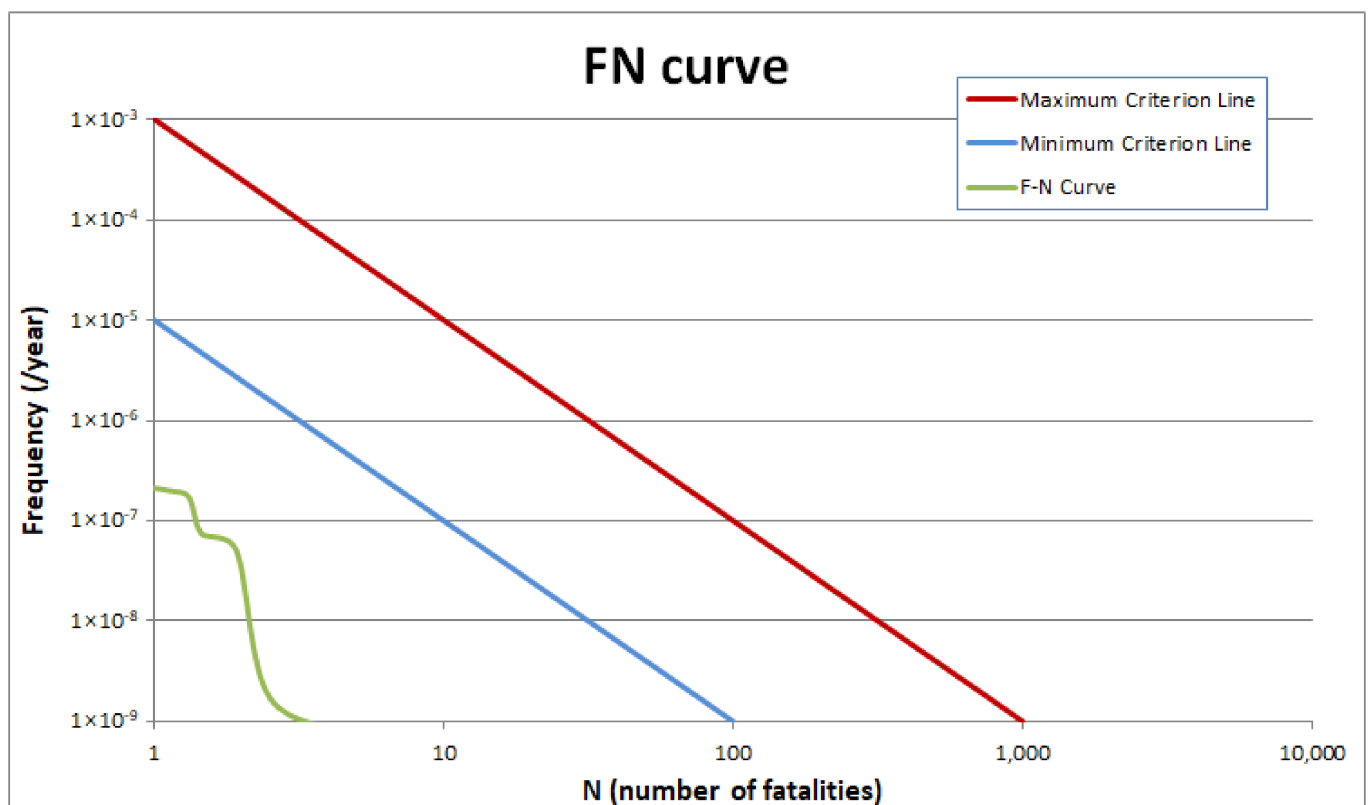


Figure 10. Societal risk (F-N curve).

The maximum number of fatalities caused by leakage and fire at the HRS was estimated to be 7.95, and the expected accident frequency was 4.60×10^{-10} /year. The F-N curve was positioned lower than the 'as low as reasonably practicable' (ALARP) level, thus demonstrating a low level of risk.

This curve did not take into account the wall protection of the HRS. Considering the existence of the wall, the default value of 0.001 was applied as the defense coefficient of the blast-wall [35]. The storage tank had a wall in 75% of directions, and the tube trailer had a wall in 25% of directions. Figure 11 shows the results of the F-N curve considering the burst-wall.

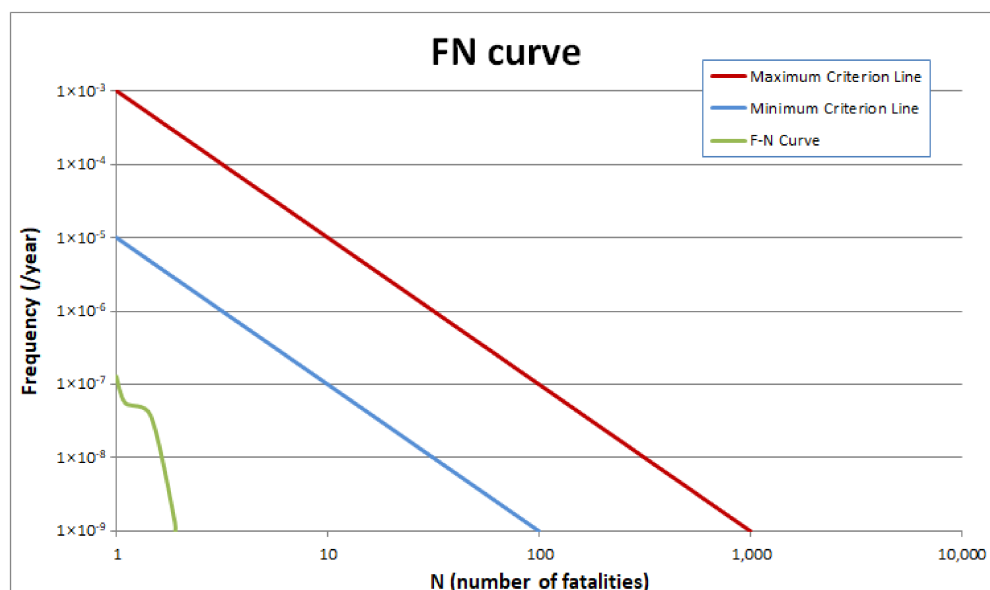


Figure 11. Societal risk (considering the wall).

4. Conclusions

This study assessed the risk range for accidents occurring at the HRS in operation and performed a safety evaluation of the HRS by assessing the societal risk; the following conclusions can be drawn.

1. Jet fire was modeled using HyRAM. The results showed that the range of fatal impact is at a maximum when a large-sized leak occurs, specifically at a distance of 27 m for a tube trailer and 22 m for a storage tank. When a medium-sized leak occurs, the distance of fatal impact is 8 m for a tube trailer and 5 m for a storage tank. When a small-sized leak occurs, there is no fatal impact.
2. The analysis performed using PHAST demonstrates a fatal impact for an overpressure radius of up to 11.08 m. The fatal impact of overpressure is not wider than that of HRS facilities. Therefore, the effect of overpressure is expected to be low in fatal effects, except for the workers of the HRS.
3. The area of the analyzed HRS is 1997 m². There is no fatal impact outside the HRS in the cases of small- and medium-sized leaks. Heat flux due to jet fire can have an effect even outside the HRS in the case of a large-sized leak, but the actual risk range may be smaller because the geographical features and firewalls of the HRS were not taken into consideration in modeling the effects of the jet fire and overpressure.

Future studies will focus on all the independent protection layers (IPLs) such as firewalls and water curtains installed at the HRS which would significantly lower the societal risk.

Author Contributions: Conceptualization, B.-i.J.; methodology, S.K.; software, B.-i.J.; validation, S.J.; formal analysis, Y.S.Y.; investigation, S.K.; writing—original draft preparation, B.-i.J.; writing—review and editing, S.J.; supervision, Y.S.Y.; project administration, S.J.; funding acquisition, S.J. All authors have read and agreed to the published version of the manuscript.

Funding: This paper was supported by the Education and Research promotion program in 2023 of Korea University of Technology & Education. This research was supported by a Korea Institute for Advancement of Technology (KIAT) grant funded by the Korean Government (MOTIE) (P0012787. The Competency Development Program for Industry Specialist).

Data Availability Statement: Not applicable.

Conflicts of Interest: The authors declare no conflict of interest.

References

1. European Parliament, EU Ban on the Sale of New Petrol and Diesel Cars from 2035 Explained. Available online: <https://www.europarl.europa.eu/news/en/headlines/economy/20221019STO44572/eu-ban-on-sale-of-new-petrol-and-diesel-cars-from-2035-explained> (accessed on 10 October 2023).
2. Ministry of Land, Infrastructure and Transport (Korea), Total Registered Motor Vehicles. Available online: <https://stat.molit.go.kr/portal/cate/statFileView.do?hRsId=58&hFormId=5409&hKeyword=%25EC%259E%2590%25EB%258F%2599%25EC%25B0%25A8%25EB%2593%25B1%25EB%25A1%259D&hTotalFlag=Y> (accessed on 19 July 2023).
3. Hydrogen Council, Hydrogen Insights 2023. Available online: <https://hydrogencouncil.com/en/hydrogen-insights-2023/> (accessed on 19 July 2023).
4. Energy Efficiency & Renewable Energy, Hydrogen Storage. Available online: <https://www.energy.gov/eere/fuelcells/hydrogen-storage> (accessed on 19 July 2023).
5. Oleszczak, P.; Wolanski, P. Ignition during hydrogen release from high pressure into the atmosphere. *Shock. Waves* **2010**, *20*, 539–550. [\[CrossRef\]](#)
6. Mogi, T.; Kim, D.J.; Shiina, H.; Horiguch, S. Self-ignition and explosion during discharge of high-pressure hydrogen. *J. Loss Prev. Process Ind.* **2008**, *21*, 199–204. [\[CrossRef\]](#)
7. Sakamoto, J.; Sato, R.; Nakayama, J.; Kasai, N.; Shibutani, T.; Miyake, A. Leakage-type-based analysis of accidents involving hydrogen fueling stations in Japan and USA. *Int. J. Hydrogen Energy* **2016**, *41*, 21564–21570. [\[CrossRef\]](#)
8. Kikukawa, S.; Mitsunashi, H.; Miyake, A. Risk assessment for liquid hydrogen fueling stations. *Int. J. Hydrogen Energy* **2009**, *34*, 1135–1141. [\[CrossRef\]](#)
9. LaFleur, A.C.; Muna, A.B.; Groth, K.M. Application of quantitative risk assessment for performance-based permitting of hydrogen fueling stations. *Int. J. Hydrogen Energy* **2017**, *42*, 7529–7535. [\[CrossRef\]](#)
10. Kikukawa, S.; Yamaga, F.; Mitsunashi, H. Risk assessment of hydrogen fueling stations for 70 MPa FCVs. *Int. J. Hydrogen Energy* **2008**, *33*, 7129–7136. [\[CrossRef\]](#)
11. Sandia National Laboratories. *Analyses to Support Development of Risk-Informed Separation Distances for Hydrogen Codes and Standards (SAND2009-0874)*; Sandia National Laboratories: Albuquerque, NM, USA; Livermore, CA, USA, 2009.
12. Korea Occupational Safety and Health Agency. *Technical Guidelines on Selection of Worst and Alternative Leakage Scenarios (P-107-2020)*; Korea Occupational Safety and Health Agency: Ulsan Metropolitan City, Korea, 2020.
13. Correa-Jullian, C.; Groth, K.M. Data requirements for improving the quantitative risk assessment of liquid hydrogen storage systems. *Int. J. Hydrogen Energy* **2022**, *47*, 4222–4235. [\[CrossRef\]](#)
14. Al-Douri, A.; Ruiz-Tagle, A.; Groth, K.M. A quantitative risk assessment of hydrogen fuel cell forklifts. *Int. J. Hydrogen Energy* **2023**, *48*, 19340–19355. [\[CrossRef\]](#)
15. Dan, S.K.; Moon, D.J.; Yoon, E.S.; Shin, D.G. Analysis of gas explosion consequence models for the explosion risk control in the new gas energy filling stations. *Ind. Eng. Chem. Res.* **2013**, *52*, 7265–7273. [\[CrossRef\]](#)
16. Chamberlain, P.; Rosicky, J.G. The effectiveness of family therapy in the treatment of adolescents with conduct disorders and delinquency. *J. Marital Fam. Ther.* **1995**, *21*, 441–459. [\[CrossRef\]](#)
17. Yüceil, K.B.; Ötügen, M.V. Scaling parameters for underexpanded supersonic jets. *Phys. Fluids* **2022**, *14*, 4206–4215. [\[CrossRef\]](#)
18. Birch, A.D.; Hughes, D.J.; Swaffield, F. Velocity decay of high pressure jets. *Combust. Sci. Technol.* **1987**, *52*, 161–171. [\[CrossRef\]](#)
19. Birch, A.D.; Brown, D.R.; Dodson, M.G.; Swaffield, F. The Structure and Concentration Decay of High Pressure Jets of Natural Gas. *Combust. Sci. Technol.* **1984**, *36*, 249–261. [\[CrossRef\]](#)
20. Ewan, B.C.R.; Moodie, K. Structure and velocity measurements in underexpanded jets. *Combust. Sci. Technol.* **1986**, *45*, 275–288. [\[CrossRef\]](#)
21. Molkov, V.; Makarov, D.; Bragin, M. *Physics and Modelling of Under-Expanded Jets and Hydrogen Dispersion in Atmosphere*; Physics of Extreme States of Matter-2009; Russian Academy of Sciences: Moscow, Russia, 2009.
22. The World Bank. *Techniques for Assessing Industrial Hazards*; World Bank Technical Paper No. 55 (WTP55); The World Bank: Washington, DC, USA, 1988.
23. Health and Safety Executive, Fire Effects. Available online: <https://www.hse.gov.uk/offshore/strategy/effects.htm> (accessed on 24 May 2023).
24. TNO. *Methods for the Determination of Possible Damage*; The Green Book (CPR16E); TNO: Toronto, ON, USA, 1992.
25. TNO. *Methods for the Calculation of Physical Effects*; The Yellow Book (CPR14E); TNO: Toronto, ON, USA, 2005.
26. CDC. Effects of Blast Pressure on Structures and the Human Body. Available online: <https://www.cdc.gov/niosh/docket/archive/pdfs/NIOSH-125/125-ExplosionsandRefugeChambers.pdf> (accessed on 24 May 2023).
27. Groth, K.M.; Hecht, E.S.; Reynolds, J.T. *Methodology for Assessing the Safety of Hydrogen Systems: HyRAM 1.0 Technical Reference Manual (SAND2015-10216)*; Sandia National Laboratories: Albuquerque, NM, USA; Livermore, CA, USA, 2015.
28. Groth, K.M.; Hecht, E.S. HyRAM: A methodology and toolkit for quantitative risk assessment of hydrogen systems. *Int. J. Hydrogen Energy* **2017**, *42*, 7485–7493. [\[CrossRef\]](#)
29. Ehrhart, B.D.; Hecht, E.S.; Groth, K.M. *Hydrogen Risk Assessment Models (HyRAM) Version 3.0 Technical Reference Manual (SAND2020-10600)*; Sandia National Laboratories: Albuquerque, NM, USA; Livermore, CA, USA, 2020.
30. RVIM. *Guideline for Quantitative Risk Assessment; Purple Book (CPR 18E)*; RVIM: Karnataka, India, 2001.

31. Ehrhart, B.; Hecht, E. *Hydrogen Plus Other Alternative Fuels Risk Assessment Models (HyRAM+) Version 4.1 Technical Reference Manual (SAND2022-5649)*; Sandia National Laboratories: Albuquerque, NM, USA; Livermore, CA, USA, 2022.
32. National Institute for Public Health and the Environment. *Method for Derivation of Probit Functions for Acute Inhalation Toxicity (RIVM Report 2015-0102)*; National Institute for Public Health and the Environment: Bilthoven, The Netherlands, 2015.
33. Health and Safety Executive, Methods of Approximation and Determination of Human Vulnerability for Offshore Major Accident Hazard Assessment. Available online: https://www.hse.gov.uk/foi/internalops/hid_circs/technical_osd/spc_tech_osd_30/spctecsd30.pdf (accessed on 23 May 2023).
34. Korea Ministry of SMEs and Startups, Commercial District Information System. Available online: <https://sg.sbiz.or.kr/godo/index.sg> (accessed on 18 June 2023).
35. General Electric, Passive IPLs. Available online: <https://www.ge.com/digital/documentation/meridium/Help/V43060/IMDQ4MDA1NTYtNTBmZS00N2Y1LThjNzQtMjY4ZTAwYWM5YmNh.html> (accessed on 18 June 2023).

Disclaimer/Publisher's Note: The statements, opinions and data contained in all publications are solely those of the individual author(s) and contributor(s) and not of MDPI and/or the editor(s). MDPI and/or the editor(s) disclaim responsibility for any injury to people or property resulting from any ideas, methods, instructions or products referred to in the content.